Accurate Free Energies of Micelle Formation†

René Pool and Peter G. Bolhuis*

van't Hoff Institute for Molecular Sciences, Universiteit van Amsterdam, Nieuwe Achtergracht 166, 1018 WV Amsterdam, The Netherlands

Received: September 29, 2004; In Final Form: November 10, 2004

We determine the free energy of micelle formation for model surfactants in a Lennard-Jones solvent by employing a hybrid semi-grand Monte Carlo simulation scheme in combination with umbrella sampling and configurational bias techniques. Comparing the results to theoretical prediction, we obtain good agreement for large micellar sizes. We also study the effect of changing the surfactant headgroup size and tail length on the critical micelle concentration. The values of and the trends in the calculated critical micelle concentrations do agree with experimental observation for nonionic surfactants. The results open up the way for the calculation of critical micelle concentrations using realistic atomic force fields.

1. Introduction

Amphiphillic surfactant molecules consisting of a hydrophilic headgroup and a hydrophobic tail can aggregate into micelles. Micelle formation of such surfactants (see Figure 1) is important for transporting oily molecules in washing processes and has received much attention from the industry. The formation of micelles has been studied extensively in the past decades by experiment,[1−6] theoretical approaches,[7−10] and computer simulation.[11−25] The qualitative origin of the formation of micelles is well understood and is akin to nucleation.[7−14] The formation of a micellar cluster is favored by the hydrophobic tails, but a surface energy penalty has to be paid leading to a nucleation barrier. In addition, the cluster size is kept finite by the decrease in configurational entropy due to the microphase separation. The result is that the free energy of formation of a single micelle shows a barrier and a well-defined minimum around the average cluster size. Several studies predict the shape of the free energy of micelle formation using molecular thermodynamic theory.[7,9,10] In particular, Chandler and co-workers recently developed an attractive theory specifying the free energy of formation of spherical micelles.[7]

A consequence of the general shape of the free energy profile is that the micellar size distribution is finite and reasonably sharply peaked. Moreover, it also follows that amphiphiles only aggregate when the driving force is large enough: when their concentration is above the so-called critical micelle concentration (CMC). The CMC is an important quantity in experimental and theoretical research of amphiphillic phase behavior and can in principle be estimated from a probability distribution of the micellar size using molecular simulation. However, although it is currently possible to perform molecular dynamics (MD) simulations using an atomistic force field[25] of micelle formation, the accessible length and time scales are relatively small. Therefore, in practice, MD simulations have to be performed far above the CMC where there is no barrier for micelle formation. To make an accurate estimate of the CMC, one has to be able to perform simulations at concentrations below or around the CMC. Using straightforward Monte Carlo (MC) simulation or molecular dynamics in combination with atomistic force fields would require huge system sizes, because many micelles have to be formed to get a reasonable size distribution. Such a large system size is accompanied by long equilibration time scales, making this simulation approach beyond current computer capabilities.

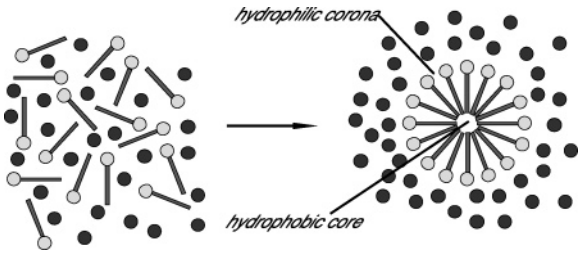

Figure 1. Micelle formation of amphiphiles. Surfactants are represented by hydrophilic heads (gray circles) with hydrophobic tails (lines). Solvent molecules are depicted by black circles.

In the past, this length and time scale problem has been circumvented by introducing various coarse-grained models for the calculation of the CMC. The simplest of these are lattice models[17−21] that provide a cheap and fast route to the qualitative behavior of surfactants. Lattice MC studies[19−21] with simple intermolecular interaction potentials reproduce CMCs within the experimental range 10^{-6}−10^{-2} M.[8,22,23] However, substantial assumptions on the nature of the interaction potentials have to be made. The assumptions are largely based on the experimental observation that oil and water do not mix. Some models set the water−water and oil−oil interactions to zero and include an effective repulsive water−oil interaction.[21,20] Others, for instance, Larson and co-workers, modeled a mixture of oil, water, and surfactant with the surfactant head and tail segments identical to water and oil beads, respectively.[18,19] Yet another model was used in a lattice grand-canonical MC (GCMC) study.[17] Here, the effective interactions between surfactant tails were attractive, whereas head−head and head−tail interactions did not contribute to the total energy. Employing the histogram reweighting method, critical micelle concentrations of two surfactants were estimated by observing a kink in the osmotic pressure, for several ranges of reduced temperatures. At low temperatures CMCs were found, corresponding to 13−14 mM in aqueous solution. The authors found that the CMC increases with increasing temperature and decreases with increasing

† Part of the special issue "David Chandler Festschrift".

10.1021/jp045576f CCC: $30.25
Published on Web 01/07/2005

chain length. These results were in qualitative agreement with experimental results of nonionic surfactants in a slightly polar medium. In all of these studies the intermolecular interactions are of the simplest form and exist only between nearest neighbor sites. Off-lattice models are slightly more realistic: the best known coarse-grained surfactant models are chain molecules on the basis of the Lennard-Jones potential, pioneered by Smit et al.[11−13] and the dissipative particle dynamics (DPD) models by Groot et al.[26,27] However, also here substantial approximations are made.

For low values of the CMC the necessary large system sizes become unwieldy, even for lattice systems. A more efficient approach for low CMCs therefore is to determine the micelle size distribution from the exact shape of the free energy as a function of the number of surfactants in a micelle. This free energy can be obtained by computer simulations of much smaller systems containing only one single micelle. A calculation of the CMC using all-atom force field simulations is still very demanding, even when using this approach. Instead, again one first has to rely on simplified (off-)lattice models to study the behavior of micelles.

In this paper, we calculate the CMC and the free energy of micelle formation for an off-lattice coarse-grained model for surfactant and solvent on the basis of the Lennard-Jones (LJ) potential. This coarse-grained potential taking into account excluded volume, van der Waals attraction, and hydrophobic interaction of all components, has been used before by several authors.[12,24,28] Although we still use a coarse-grained potential, this approach, in principle, opens up the way for the prediction of CMCs for surfactants using atomistic force fields.

To obtain the free energy profile as a function of micelle size, we employ the isobaric semi-grand canonical MC (SGCMC) sampling method[29] in combination with umbrella sampling. Imposing a chemical potential difference $\Delta\mu$ between surfactants and solvent, the SGCMC method allows for the transformation of solvent molecules into surfactants and vice versa. The combination with umbrella sampling enables us to sample the entire size probability distribution of a single micelle. Efficiency is further increased by making use of the configurational bias Monte Carlo technique to grow chain molecules in dense solutions.

The SGCMC method was used in two earlier studies on amphiphile solutions. Kusaka and Oxtoby used diatomic surfactant and solvent molecules that interacted via the LJ potential.[24] To obtain amphiphillic behavior, solvent−tail and head−tail interactions were made less attractive than head−head and solvent−solvent interactions, by adjusting the LJ epsilon parameter. Above the CMC, estimated around 666 mM, the free energy barrier for micellization was at most 6 k_BT. In the other study, by one of the present authors, the solvent was represented by hard spheres and surfactants by linear molecules with a headgroup identical to a solvent molecule.[14] The surfactant had a stiff infinitely thin rodlike tail. The calculated free energy profile in ref 14 shows a minimum, and a large barrier between the single surfactant and the micelle, indicating a stable micelle solution. The corresponding CMC was 6.3×10^{-8} mM in aqueous solution. This low value was caused by the highly nonadditive nature of the surfactant model. In the current work we use a similar sampling method, but with a more realistic LJ based model.

The paper is organized as follows: In section 2 we briefly review a recent theory for micellization. The semi-grand SGCMC technique for the calculation of the free energy is given in section 3. In section 4 we introduce the model. The results of the free energy calculation are given in section 5 and we end with conclusions.

2. Theory of Micelle Formation

Molecular-thermodynamical theories offer a precise framework for the process of micelle formation.[30] In the past decades, several authors have contributed significantly to this field. For instance, the extensive theoretical treatment of micellization by Nagarajan and Ruckenstein,[10] and also the earlier work of Puvvada and Blankschtein[9] lay out the different contributions to the free energy in terms of micelle size. Optimizing the total free energy of micellization then leads to predictions of, e.g., the critical micelle concentration. More recently, Maibaum, Dinner, and Chandler[7] introduced an alternative approach to the free energy of micellization, which is more accessible and concise. In this section we will briefly summarize this theoretical approach.

The natural way to view a micelle solution is as a multiphase coexistence in which micelles are in equilibrium with a solution of single surfactants. If we consider an almost ideal solution, then equilibrium concentrations are only determined by the free energy difference ΔG_n between a micelle of n surfactants and a solution of single surfactants

$$\exp[-\beta\Delta G_n] = [\rho_n\sigma^3]/[\rho_1\sigma^3]^n \quad (1)$$

where $\beta = 1/k_BT$ is the inverse temperature with k_B Boltzmann's constant and T the temperature, ρ_n is the density of clusters of size n and σ is a molecular size parameter. The crossover between single surfactants and micelles (the CMC) takes place when[7]

$$\ln[\rho_1\sigma^3] \approx \beta\Delta G_n/n \quad (2)$$

The free energy difference $\Delta G_n = f_n - nf_1$ between a micelle of n surfactants (f_n) and a solution of single surfactants (nf_1) is given by the sum of three terms.

$$\Delta G_n = -\mu_{\text{trans}}n + 4.8\gamma(n\delta\sigma^2)^{2/3} + 0.75(\sigma/\delta)^{4/3}n^{5/3}k_BT \quad (3)$$

The first is the free energy μ_{trans} needed to transfer a surfactant from the core of the micelle to the solvent. The second contribution is the interfacial free energy $4\pi\gamma R^2 \approx 4.8\gamma(n\delta\sigma^2)^{2/3}$, where γ is the oil−water surface tension and R is the radius of the micelle, δ is the typical length over which hydrophobic, and hydrophilic parts are separated. The last part is the loss of entropy connected with the fact that the hydrophilic headgroups are restraint to the micelle surface. This term is estimated $S_n \approx -0.75(\sigma/\delta)^{4/3}n^{5/3}k_B$.[7]

The first contribution in eq 3 is negative whereas the latter two are positive. The sum of these contributions gives rise to a minimum in the free energy of micelle formation. The optimal micelle size will be reached at a surfactant number n that minimizes the free energy per surfactant $\Delta G_n/n$. For more details on this approach we refer the reader to ref 7. In section 5.2 we compare our simulation results to these theoretical predictions. As both the simulation and the theory focus on the free energy it is natural to compare our results with a molecular thermodynamic theory. Here, we restrict ourselves to the theory of Chandler et al. (i.e., eq 3), although the comparison to other theoretical work[9,10] would certainly be possible.

3. Simulation Methods

To estimate the free energy profile for micelle formation as a function of micelle size by computer simulation, we employ

an isobaric semi-grand hybrid MC scheme with configurational bias Monte Carlo swap moves in combination with umbrella sampling. In the next few paragraphs we explain the several techniques in detail.

3.1. Semi-grand Ensemble. We could estimate the micelle free energy as a function of cluster size by computing the chemical potential of adding a surfactant to an existing micelle for every cluster size. However, this is very expensive because many simulations have to be performed. A better option is the isobaric grand canonical ensemble in which the number of surfactants is allowed to vary but the number of solvent molecules is kept constant. When the simulation is restricted to a single micellar cluster in the system, one can determine the micelle distribution at a particular chemical potential. The use of biasing techniques such as umbrella sampling allows visiting the unlikely regions in the size probability distribution. However, using grand canonical simulations, the probability of adding a surfactant to a dense liquid is still very low. To increase the insertion probability, we make use of the semi-grand canonical MC(SGCMC).[29,31] In the SGCMC technique one imposes a chemical potential difference $\Delta\mu$ between different species, instead of the absolute chemical potentials. The isobaric semigrand potential $Y(N,\Delta\mu,p,T)$ of a binary mixture of surfactant chains (c) and solvents (s) is defined by the Legendre transform between the variables n (number of surfactant molecules) and $\Delta\mu = \mu_c - \mu_s$ of the usual Gibbs free energy:[32]

$$Y = G - n\Delta\mu = \mu_s N \tag{4}$$

$$dY = -S\,dT + V\,dp - n\,d\Delta\mu + \mu_s\,dN \tag{5}$$

where $N = n + n_s$ denotes the total number of particles with n_s the number of solvent particles, and V is the volume. The corresponding partition function is given by[29]

$$\Xi_{SG} = \frac{\beta p}{N!\Lambda^{3N}}\int dV \exp[-\beta pV]V^N \times \sum_{\text{identities}} \exp[\beta n\Delta\mu] \times \int d\boldsymbol{s}^N \exp[-\beta U(\boldsymbol{s}^N)] \tag{6}$$

where p is the pressure and Λ the thermal wavelength of the solvent particles. The sum is over the particle identities, rather than all compositions.[29] In a simulation we can impose the chemical potential difference $\Delta\mu$ between surfactant and solvent by choosing a molecule randomly and trying to *change* its identity, e,.g. a solvent molecule s to a surfactant molecule c. The Metropolis acceptance rule for randomly selecting a particle and changing it from a solvent to a surfactant is

$$P_{acc}(s\rightarrow c) = \min[1, \exp\{-\beta\Delta U_{s\rightarrow c} + \beta\Delta\mu\}] \tag{7}$$

where $\Delta U_{s\rightarrow c}$ is the energy difference involved in changing species.[14] The min function returns the smaller of its arguments. The Monte Carlo move for changing species, in principle greatly speeds up the sampling of the phase space.[31]

3.2. Configurational Bias MC. Because we are trying to insert a chain molecule, the insertion probability decreases exponentially with the number of beads in the chain. We can increase the insertion acceptance probability using the Configurational Bias MC (CBMC) method, which was especially devised for polymers.[29] In ordinary CBMC the first polymer segment is inserted randomly. The subsequent segments are grown in a biased fashion, with each segment selected from a set of trial positions with a probability proportional to the Boltzmann distribution, favoring the position having the lowest energy. The bias has to be corrected after the insertion to obey detailed balance, but the acceptance probability of the new configuration is much higher than just some randomly inserted configuration.[29]

In our approach the first segment (the surfactant headgroup) comes in the place of the selected solvent molecule. The tail of length l is grown in the usual way by generating a set of k trial positions. The acceptance rule for a Monte Carlo move involving the change from a solvent molecule s to a surfactant chain c is

$$P_{acc}(s\rightarrow c) = \min[1, \exp\{\beta\Delta\mu + \beta\Delta U_{s\rightarrow h}\}W^{(n)}] \tag{8}$$

where $\Delta U_{s\rightarrow h} = U_h - U_s$ is the energy difference involved in changing the solvent to a headgroup h. $W^{(n)} = \prod_{i=1}^{l} w_i$ is the Rosenbluth factor for the newly inserted tail, with $w_i = \sum_{j=1}^{k} e^{-\beta U_j}$, where U_j is the total energy of the jth trial prosition of the ith bead. A trial tail-bead is selected with a probability $p_i = e^{-\beta U_i}/w_i$. Similarly, a change from surfactant to solvent is accepted according

$$P_{acc}(c\rightarrow s) = \min\left[1, \exp\{-\beta\Delta\mu - \beta\Delta U_{s\rightarrow h}\}\frac{1}{W^{(o)}}\right] \tag{9}$$

with $W^{(o)}$ the Rosenbluth factor for the old chain configuration, calculated in the same way as $W^{(n)}$ but with only $k-1$ random trial positions, and including the old position of the ith bead as the kth position.[29]

As the solubility of surfactants is low in the bulk solvent, we attempt s $\rightarrow$ c and c $\rightarrow$ s moves only inside a shell surrounding the micelle. This is achieved as follows. We randomly select a molecule from our system. If this is a solvent, an expensive swap move is only attempted if it is at a distance smaller than $r_{shell} = r_{max} + d_{shell}$ from the micelle center of mass, where r_{max} is the maximum micelle radius (defined as half the largest head−head distance within the micelle) and d_{shell} is the input shell thickness (typically 1.5 σ_s). Before accepting the swap move, we check if the position of the headgroup of the trial surfactant is still within r_{shell} of the new micelle center of mass to obey detailed balance. If the randomly selected molecule is a surfactant, it is by definition within the micelle shell. Before entering the swap procedure, we calculate the center of mass of the micelle without the selected surfactant and check if the solvent (at the headgroup position) is still within the micelle shell.

3.3. Isobaric Hybrid MC. In addition to an efficient insertion algorithm to ensure a fixed chemical potential difference, proper sampling also demands thermal equilibrium. In a Monte Carlo simulation, this is ensured by particle displacements. For our system, the Metropolis method for particle displacements[33] is not the most efficient method for reaching equilibrium. By employing molecular dynamics (MD) less computational effort is required to reach equilibrium, due to the collective nature of particle displacements in MD.[29,34] Therefore, we employ a hybrid MC scheme and use several MD steps as a translational MC move. These steps are performed at constant temperature using the Andersen thermostat.[35] Additionally, we require a constant pressure to allow the micelle to grow without raising the pressure. Therefore, during the sampling we occasionally, at random intervals, perform volume change MC moves.[29]

3.4. Determination of the CMC. In principle, by using the CBMC semigrand algorithm, the micellar size distribution $P(n,\Delta\mu)$ can be obtained as a function of micellar cluster size n. However, biasing techniques such as umbrella sampling have to be invoked to obtain sufficient statistics in the unlikely regions of the size distribution.[14] We obtained the entire distribution at

a certain $\Delta\mu^{sim}$ by restricting the semigrand simulation to windows with a hard boundary and by applying a biasing function $B(n,\Delta\mu^{sim})$, tuned to flatten the measured distribution $P_{sample}(n,\Delta\mu^{sim})$ during the sampling. In the analysis of the results this biasing function is added again to the size distributions, so that the final unnormalized size distribution for $\Delta\mu^{sim}$ is

$$P(n) = P_{sample}(n,\Delta\mu^{sim}) \exp[B(n,\Delta\mu^{sim})] \quad (10)$$

From this distribution the single micelle free energy profile this $G(n)$ can be calculated by

$$G(n) = -k_B T \ln P(n,\Delta\mu^{sim}) + n\Delta\mu^{sim} + \text{constant} \quad (11)$$

Once this $G(n)$ is known, we can calculate the distributions for every value of $\Delta\mu$ by simply inverting eq 11

$$P(n,\Delta\mu) = \exp[-\beta G(n) + n\beta\Delta\mu]/Q \quad (12)$$

where $Q = \sum\exp[-\beta G(n) + n\beta\Delta\mu]$ is a normalizing constant. To estimate the CMC from this distribution requires a proper definition of the CMC. Here we define the CMC as the surfactant concentration at which half of the surfactants is isolated and the other half is in aggregated form:[14]

$$P(1,\Delta\mu) = \sum_{i=2}^{M} iP(i,\Delta\mu) \quad (13)$$

where M is the aggregation number above which the micelle breaks up into two aggregates. Although this definition is slightly arbitrary, the CMC is not very sensitive to this definition. Solving eq 13 yields $\Delta\mu^{CMC}$, which in turn leads to the surfactant number density at the CMC ρ^{CMC} by

$$k_B T \ln\left[\frac{\rho^{CMC}}{\rho_s}\right] = \Delta\mu^{CMC} - \Delta\mu^{ex} \quad (14)$$

The excess chemical potential difference $\Delta\mu^{ex}$ between surfactant and solvent has to be determined in a separate simulation at constant *NVT*, by means of the Widom particle insertion technique. Also here we make use of the CBMC algorithm.[29]

4. Surfactant Model

We base our surfactant model on the truncated and shifted Lennard-Jones potential. To allow variety in the strength of attraction between two particles of species i and j, we use a species dependent LJ potential

$$\phi^{LJ}(r_{ij},\epsilon) = 4\epsilon\left[\left(\frac{\sigma_{ij}}{r_{ij}}\right)^{12} - \left(\frac{\sigma_{ij}}{r_{ij}}\right)^{6}\right] \quad (15)$$

where r_{ij} is the distance between two particles of species i and j, σ_{ij} is the range of interaction of the potential for two species i and j, and ϵ is the depth. The interaction range parameters σ_{ij} were calculated from the standard mixing rule $\sigma_{ij} = {}^1/_2(\sigma_i + \sigma_j)$,[36] where σ_i and σ_j are the particle sizes of species i and j, respectively. To avoid tail corrections, we truncate the potential at a cutoff $r_c = 2.5\ \sigma_{ij}$, and shift it to obtain a smooth potential at the cutoff

$$\phi^{TS}(r_{ij},\epsilon) = \begin{cases} \phi^{LJ}(r_{ij},\epsilon) - \phi^{TS}(r_{ij},\epsilon) & r_{ij} \le r_c \\ 0 & r_{ij} > r_c \end{cases} \quad (16)$$

Throughout this paper we use reduced units. The reduced unit of energy is ϵ, of length σ, of density σ^{-3}, of pressure $\sigma^{-3}\epsilon$, and of temperature ϵ/k_B. The solvent molecules s are modeled by standard ($\epsilon_s = \epsilon$, $\sigma_s = \sigma$) LJ particles. The surfactants c consist of a chain of LJ particles (a headgroup h and tail beads t) linked together by a harmonic potential (see Figure 2).

Figure 2. Cartoon of surfactant h_1t_4. The hydrophobic tail beads (dark circles) and the hydrophilic head (light circle) are connected by harmonic springs.

TABLE 1: Interaction Parameters for the Model Surfactants[a]

r_c/σ_{ij}	s	h	t
s	2.5	2.5	$2^{1/6}$
h	2.5	$2^{1/6}$	$2^{1/6}$
t	$2^{1/6}$	$2^{1/6}$	2.5

surfactant	name	σ_s	σ_h	σ_t
A	h_1t_4	1.0	1.0	0.5
B	h_1t_4	1.0	1.5	0.75
C	h_1t_4	1.0	1.5	1.0
D	h_1t_4	1.0	2.0	1.0
E	h_1t_5	1.0	2.0	1.0

[a] Top: values for the cutoff radius r_c in terms of the size parameter $\sigma_{ij} = (\sigma_i + \sigma_i)/2$ for the solvent (s), headgroup (h), and tail bead (t). Truncating and shifting at $r_c = 2^{1/6}\ \sigma_{ij}$ leaves only the repulsive part of the LJ potential; at $r_c = 2.5\ \sigma_{ij}$ the attractive part is considered as well. Bottom: size parameters for surfactants A−E. All values in reduced units.

$$\phi^{harm}(r_{ij}) = \frac{1}{2}k_{harm}(r_{ij} - r_{eq})^2 \quad (17)$$

where r_{eq} is the average equilibrium distance between beads and k_{harm} is the spring constant. The harmonic equilibrium distance was set to $r_{eq} = \sigma_{ij}$ and the spring constant was set to $k_{harm} = 5000$, ensuring that 98% of the bond lengths were within 2% of the average value of r_{eq}.[11]

Many values for the interaction parameters in the LJ model will induce surfactant behavior, as long as the tail-beads behave "oil-like" and the head-beads "water-like". One requirement is that the surfactant tail should "dislike" the solvent and the headgroup. This can be reproduced, for instance, by the setting the cutoff radius $r_c = 2^{1/6}\ \sigma_{ij}$, the minimum in the potential, thus only retaining the repulsive part of the LJ potential (better known as the WCA potential[37]). However, the parameters should also be such that spherical micelle formation is favored. In particular, the size of the headgroup should be large enough so that spherical micelles are preferred instead of other topologies.[8]

In Table 1 we give the r_c interaction parameters used in this work. The r_c values effectively induce hydrophillicity of the surfactant head and hydrophobicity of the tail. This parameter set was successfully employed by Smit et al. to simulate micelle formation of h_3ht_5 surfactants,[12] consisting of a linear tail with a tetrahedral headgroup. These interaction parameters were in turn based on an earlier model by Telo da Gama and Gubbins[38] and were also used in refs 11−13. In the study of Smit et al.[12] micelles were formed from a surfactant/solvent mixture at $T = 2.2\ \epsilon/k_B$ and $\rho = 0.7\ \sigma^{-3}$. The cluster size distribution showed an optimal micelle size of 20−25 surfactants. Using the same parameters we can expect similar micelle sizes in our simulations.

Smit et al. used the complex h_3ht_5 geometry,[12] but we can obtain the same surfactant behavior with a simpler linear surfactant containing only one bead per headgroup. To obtain spherical micelles the headgroup needs to be significantly larger

in size than the tail beads.[8] We achieve just that by changing the σ_h/σ_t ratio. The headgroup size of our surfactants should be about 1.5−2.0 times as large as a tail-bead. We modeled a h_1t_4 surfactant with one headgroup and four tail beads, using four different head and tail particle sizes (denoted A−D) and a h_1t_5 surfactant with five tail groups denoted E (see Figure 2 and Table 1). For surfactant h_1t_4 we obtain spherical micelles only when using bulky headgroup, for instance, when $\sigma_h = 2\sigma_t$.

The choice for the interaction range parameters σ_{ij} has consequences for the mapping of the coarse-grained potential on realistic systems. Although the diameter of the tail bead in surfactant B is only 75% of that of the solvent, its volume is about 2.4 times as small. Assuming that one tail bead consists of three CH_2 groups (which is reasonable if we want to compare to experimental surfactants), we can say that there are approximately seven waters in one solvent bead, which is rather high. Surfactant B is simulated at $\langle\rho_s\rangle = 0.7\ \sigma_s^{-3}$ (see section 5), resulting in a molecular length scale of $\sigma_s \approx 5.3 \times 10^{-10}$ m, given that water has a density of $\rho_{H_2O} = 55.5 \times 10^3$ mol·m^{-3} at room temperature. The average separation between a carbon atom at position m and a carbon atom at position $m + 4$ in a linear alkane is 3.8 Å. This distance should correspond to the bead separation in the tails $\sigma_t = 0.75$ and $\sigma_s \approx 4.0$ Å. Hence, the coarse-graining of surfactant B is reasonable. The tail particles of surfactants C−E have the same size as the solvent particles. For these surfactants we also use a coarse-graining mapping of three CH_2 groups per tail bead and for the solvent three waters per bead. The surfactants C−E were simulated at $\langle\rho_s\rangle = 0.6\ \sigma_s^{-3}$ (see section 5), giving a length scale of $\sigma_s = \sigma_t \approx 3.8$ Å, also a very reasonable value.

The diameter of a tail bead of surfactant A is twice as small as that of a solvent particle, making the sampling size distribution much faster than for the other surfactant. Although the size ratio seems a bit unrealistic for nonionic surfactants with alkane tails in water, we can use the results for surfactant A to compare with theory.

5. Results and Discussion

5.1. CMC. For surfactants A and B, the simulations were carried out at $T = 1.0$, $N = 2880$, and $p = 0.6$. This pressure corresponds to a solvent density of $\rho_s = 0.7$, well within the liquid region of the truncated and shifted LJ phase diagram.[29] For surfactants C−E, we imposed a pressure of $p = 0.13$ with a corresponding density of $\rho_s = 0.6$. This density is still within the liquid region of the truncated and shifted LJ phase diagram. The micellar size distribution was sampled in the semi-grand canonical isobaric ensemble using umbrella sampling, as described in section 3. Dividing the entire range of micellar sizes $n = 0$−60 into several windows of around 10 units, we performed independent sampling for each window. The application of a biasing potential in each window ensures that all micelle sizes in the window were equally frequently visited, which enhances the statistics significantly. Afterward, this bias was removed by reweighting the observed distribution using eq 10. The biasing function itself can be obtained by an iterative procedure. First, we performed an unbiased simulation and obtained an estimate for the free energy from the resulting distribution using eq 11. The negative of this free energy function was then used as a biasing potential in the next iteration. To obtain good statistics, we repeated this procedure until the sampling distribution was almost uniform. Finally, the data sets for all windows were fitted simultaneously to the same sixth-order polynomial using the additive constant of eq 11 as an additional fitting parameter.[39]

The excess chemical potential difference $\Delta\mu^{ex}$ between surfactant and solvent was determined in a separate simulation at constant *NVT* using the Widom insertion method.[29] Because the density of the solvent is that of a liquid, we can expect that the surfactant solubility is low.

The single micelle free energies as a function of aggregation number for all surfactants at the computed $\Delta\mu^{CMC}$ are plotted in Figure 3. These curves all show a barrier between the single surfactant and the micelle. Figure 3 also shows the corresponding size distributions, which have shapes typical for micelles. For surfactants A and B the most probable micelle size is 20−25 surfactants. This size is $n \approx 20$ and $n \approx 30$ for surfactants D and E, respectively. The optimal micelle size of surfactant D is lower than that of A and B, although the head to tail size ratio is the same. Though this difference could be caused by the different imposed pressures, it is more likely that the relatively smaller solvent particles penetrate deeper into the micelle, and effectively increase the headgroup−headgroup repulsion, thus giving rise to smaller optimal micelle sizes.

For surfactant C there seems to be no well-defined free energy minimum at $\Delta\mu^{CMC}$. Instead, we observed break up of aggregates above size 50, indicating that aggregates of surfactant C are not very stable. This behavior is due to the geometry of the surfactant. If the headgroup is too small compared to the tail bead size, a spherical micelle is unstable and other geometries such as cylinders are preferred.[8] This instability is further illustrated in Figure 4, where we plot the positions of the headgroups inside a micelle as a function of the distance r to the center of mass of the micelle. The headgroups in micelles consisting of surfactants A or B are confined to a distinct value of r, whereas the headgroups in a micelle made up of surfactant C are much less ordered. These micelles are also prone to more shape fluctuations.

In Table 2 we list the calculated CMCs for all surfactants as well as the excess chemical potential differences $\Delta\mu^{ex}$ between the solvent and the surfactants. Interestingly, the calculated CMCs lie within the experimental range of nonionic surfactants, provided one assumes three CH_2 groups per tail bead. At first sight it seems strange that $\Delta\mu^{ex}$ for surfactant D is lower than that of surfactant C as the headgroup is larger. However, if σ_h is increased, not only the repulsive range of the interaction potential is increased but also the attractive part, leading to a lower value of μ^{ex}. The computation of $\Delta\mu^{ex}$ is prone to significant statistical errors due to the difficulty of insertions during the Widom procedure. It is this statistical error that largely determines the error in the CMC, rather than that of the free energy profile.

The CMCs of surfactants A and B were determined from simulation data at the same pressure and thus at almost the same solvent density. Surfactant B is larger than A and should therefore have lower solubility in the LJ fluid. As a result its CMC should also be lower than that of surfactant A. This is confirmed by the simulation results: surfactant B has a 7-fold lower CMC than surfactant A. One would expect the even larger surfactant C to have a lower CMC than B. However, surfactant C was simulated at a lower pressure(density) and has therefore a higher solubility. The higher CMC of about 5 times that of surfactant B, is probably caused by this effect. Comparing the CMC values for surfactant C−E (which were determined under the same conditions), we can conclude that increasing the head size of the surfactant results in a higher CMC, whereas increasing the tail length lowers the CMC.

These trends are also observed in experiments. Huibers et al. discussed experimental CMCs of 77 nonionic surfactants,[23]

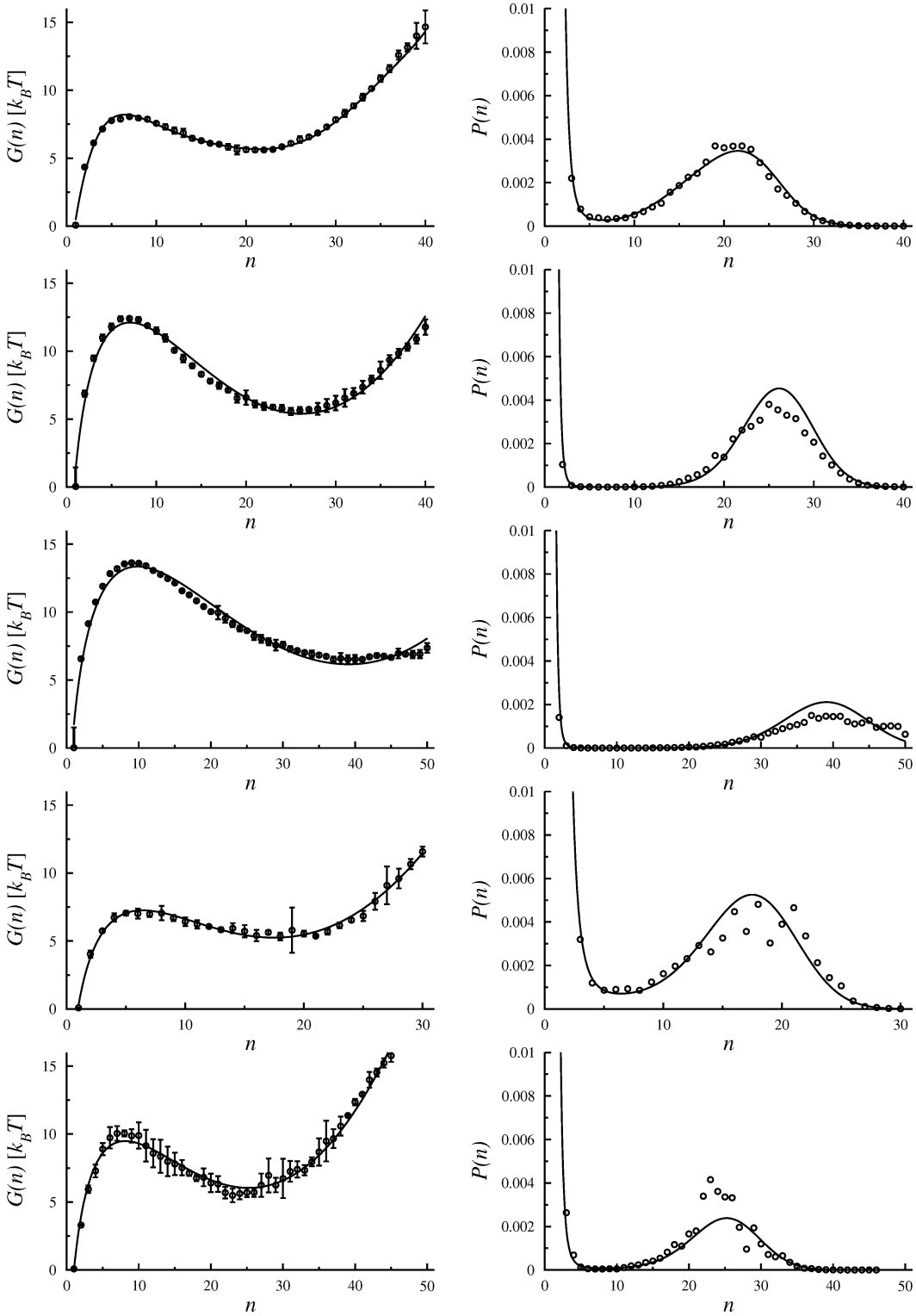

Figure 3. Left: free energy profiles of a single micelle at the CMC as a function of number of surfactants (aggregation number) *n*. Right: a zoom in on the corresponding micellar size distribution. From top to bottom the curves correspond to surfactant A−E. The solid lines are the nonlinear fit to the theory by Chandler et al.[7] See section 5.2.

of which we list a small selection in Table 3. These linear surfactant have a relatively small but bulky headgroup, and as such mostly resemble our model surfactants. Assuming three CH_2 groups per tail bead we can map the h_1t_4 surfactant on a C12 surfactant, and the h_1t_5 on a C15 surfactant. The simulated CMCs lie all within the experimental range. If we consider increasing tail length by going from C12 to C15 while keeping the same headgroup, we see a decrease in the CMC, which is reproduced by our results. Increasing the size of the headgroup from C12E3 to C12E8 increases the CMC, a trend that is also seen in our simulations. We are aware that comparing simulation results to these experimental CMCs is dangerous, as our coarse-grained potentials and conditions do not necessarily reproduce all relevant properties of the experimental surfactant. In particular, we cannot expect the simple LJ solvent at our reduced temperatures and pressure to reproduce liquid water at ambient conditions. Also, it is not clear that the average micellar size, or aggregation numbers we obtain in the simulations are present

TABLE 2: Chemical Potential Differences at the CMC and Corresponding CMCs for the Surfactants Studied[a]

surfactant	name	σ_h	σ_t	$\Delta\mu^{ex}$	$\Delta\mu^{CMC}$	ρ^{CMC}	CMC (M)
A	h_1t_4	1.0	0.5	12.0(1)	0.2	$5.3(5) \times 10^{-5}$	$4.2(4) \times 10^{-4}$
B	h_1t_4	1.5	0.75	14.6(6)	0.8	$7(4) \times 10^{-7}$	$6(3) \times 10^{-5}$
C	h_1t_4	1.5	1.0	9.6(1)	−2.5	$3.3(3) \times 10^{-6}$	$3.1(3) \times 10^{-4}$
D	h_1t_4	2.0	1.0	7.5(1)	−4.2	$5.0(5) \times 10^{-6}$	$4.6(5) \times 10^{-4}$
E	h_1t_5	2.0	1.0	8.2(2)	−5.7	$6(1) \times 10^{-7}$	$5(1) \times 10^{-5}$

[a] Using the Widom[41] insertion method, the solvent excess chemical potentials were estimated $\beta\mu_s^{ex} = -2.0$ and $\beta\mu_s^{ex} = -2.5$ for the LJ fluid at $\rho_s = 0.7\ \sigma_s^{-3}$ and $\rho_s = 0.6\ \sigma_s^{-3}$, respectively. The error in the last decimal is given in parentheses.

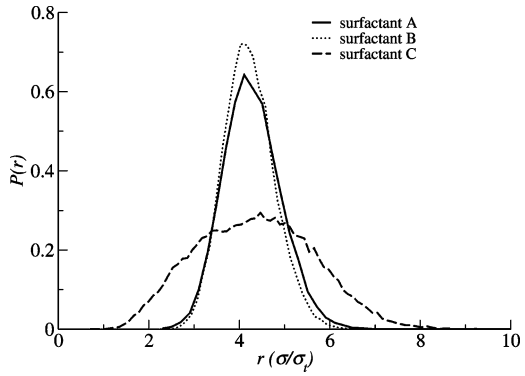

Figure 4. Distribution of the probability to find a head particle of surfactants A−C at a distance r from the micelle center of mass. This figure was obtained from MD simulations of micelles at constant NpT with 24 surfactants in 2586 solvents.

TABLE 3: Experimental CMCs at $T = 298$ K

surfactant	CMC (M)	ref
linear alkylethoxylates		
decyl triethylene oxide (C10E3)	6.0×10^{-4}	1
dodecyl diethylene oxide (C12E2)	3.3×10^{-5}	2
dodecyl triethylene oxide (C12E3)	5.2×10^{-5}	3
dodecyl octaethoxylate (C12E8)	1.0×10^{-4}	4
pentadecyl octaethoxylate (C15E8)	3.4×10^{-6}	42
alkanediols		
1,2-decanediol (C10DIOL)	2.3×10^{-3}	5
1,2-dodecanediol (C12DIOL)	1.8×10^{-4}	6
1,3-pentadecanediol (C15DIOL)	1.3×10^{-5}	7
alkyl glucose ethers		
n-dodecyl-β-D-glucoside (C12GLUC)	1.9×10^{-4}	3
sucrose monolaurate (C12SUCR)	3.4×10^{-4}	6

in experimental micelles. Nevertheless, this exercise shows that simulated surfactant CMCs can in principle be mapped on real surfactants. We hope that the use of realistic atomistic potentials will make a quantitative comparison without adjustable parameters possible in the future.

5.2. Comparison with Theory. To compare our simulation results with the recent Maibaum−Dinner−Chandler theory[7] for the free energy of micelle formation, we performed a nonlinear fit of eq 3 to our data. Using the basic form $G(n) = a_0 + a_1 n + a_2 n^{2/3} + a_3 n^{5/3}$, we obtained the coefficients a_i which in turn determined the free energy of transporting a surfactant from the water phase to the oil phase μ_{trans}, the characteristic surfactant length-scale δ/σ and the oil−water surface tension γ. The fits are shown in Figure 3 as solid lines, and the fitted values for μ_{trans}, the ratio δ/σ, and the surface tension γ are presented in Table 4. When surfactants A−E are fully extended, their lengths are $4.5\sigma_t$, $4.5\sigma_t$, $4.25\sigma_t$, $4.5\sigma_t$, and $5.5\sigma_t$ respectively. The δ/σ parameter in Chandlers theory should be about half that value, $\delta/\sigma \approx 2.25$. For all surfactants we found a δ/σ which is comparable to that value. At room temperature, the oil−water surface tension is $\gamma = 51$ mN/m.[40] If we use the length scale for the tail beads of about $\sigma_t \approx 4$ Å (cf. section 4), we obtain oil−water surface tensions γ that are more or less comparable to the experimental value for surfactant models A, C, and E. The values for surfactants B and D are too high. However, the fits are rather sensitive to the value of the surface tension. When the surface tension is fixed at a constant value of $\gamma = 51$ mN/m, the nonlinear fits to our free energy curves become worse, but the fitted values for the $\mu_{trans} \approx 7.2$ and the $\delta/\sigma \approx 2.4$ parameter are much more consistent.

TABLE 4: Fitting the Free Energy Curves to the Theory of Maibaum et al.[7,a]

surfactant	name	μ_{trans} (k_BT)	δ/σ	γ (mN/m)
A	h_1t_4	8.4	2.0	70.9
B	h_1t_4	11.8	1.6	115.8
C	h_1t_4	7.4	2.8	57.5
D	h_1t_4	10.1	1.6	94.2
E	h_1t_5	8.9	2.1	76.8

[a] The basic parameters in eq 3 are obtained by fitting the free energy curves from Figure 3 using a nonlinear fit procedure. The estimated fit value of the oil−water surface tension γ at room temperature can be compared to the experimental value $\gamma = 51$ mN/m.[40]

On the other hand, the Maibaum−Dinner−Chandler theory is only valid in the large n limit ($n \approx 100$), and thus does not necessarily predict the correct free energy form for our simulations, which are done for relatively small micelle size ($n < 50$). The worse fits either indicate that n is not large enough in our simulation or that the surface tension of our Lennard Jones system is not equal to that of water−oil. However, for surfactant C−E the only difference is the headgroup size or the tail length, so the surface tension should be the same in these cases. The fit is worst for surfactant D, which also has the smallest aggregation number. The conclusion must be that the theory becomes less accurate for surfactant D where $n = 20$, whereas it is better for C and E ($n > 30$).

6. Conclusion

In summary, we have shown that the CMC can be determined accurately for coarse-grained LJ-type surfactants in a solvent, by computing the free energy of a single micelle as a function of aggregation number employing the isobaric SGCMC ensemble in combination with CBMC and umbrella sampling. We also obtained a micellar size distribution from the free energy of micelle formation. The applied method is more efficient than conventional MC or MD methods that require large system sizes and long equilibration times. The calculated CMCs are within the range of experimental values. Increasing the headgroup size gives a higher CMC and increasing surfactant tail length lowers the CMC, two trends that are also seen in experiment. Comparison of our free energies to the Maibaum−Dinner−Chandler theory reveals that the theory, which was developed for large aggregation number, agrees best for the surfactant systems showing large micelles.

We believe that the method presented here can be extended to simulations using more realistic water potentials in combination with united atom alkane models, to incorporate effect of hydrophobicity more accurately.

Acknowledgment. We thank Berend Smit and David Dubbeldam for a critical reading of the manuscript. P.G.B. acknowledges financial support from the organization for Fundamenteel Onderzoek der Materie (FOM).

References and Notes

(1) Corkill, J. M.; Goodman, J. F.; Harrold, S. P. *Trans. Faraday Soc.* **1964**, *60*, 202.
(2) Shinoda, K.; Yamanaka, T.; Kinoshita, K. *J. Phys. Chem.* **1959**, *63*, 648.
(3) Shinoda, K.; Yamaguchi, T.; Hori, R. *Bull. Chem. Soc. Jpn.* **1961**, *34*, 237.
(4) Rosen, M. J.; Cohen, A. W.; Dahanayake, M.; Hua, X. Y. *J. Phys. Chem.* **1982**, *86*, 541.
(5) Kwan, C.-C.; Rosen, M. J. *J. Phys. Chem.* **1980**, *84*, 547.
(6) Herrington, T. M.; Sahi, S. S. *Colloids Surf.* **1986**, *17*, 103.
(7) Maibaum, L.; Dinner, A. R.; Chandler, D. *J. Phys. Chem. B* **2004**, *108*, 6778.
(8) Isrealachvilli, J. N. *Intermolecular and Surface Forces*, 2nd ed.; Academic Press: London, U.K., 1992.
(9) Puvvada, S.; Blankschtein, D. *J. Chem. Phys.* **1990**, *92*, 3710.
(10) Nagarajan, R.; Ruckenstein, E. *Langmuir* **1991**, *7*, 2934.
(11) Smit, B.; Hilbers, P. A. J.; Esselink, K.; Rupert, L. A. M.; van Os, N. M.; Schlijper A. G. *J. Phys. Chem.* **1991**, *95*, 6361.
(12) Smit, B.; Esselink, K.; Hilbers, P. A. J.; van Os, N. M.; Rupert, L. A. M.; Szleifer, I. *Langmuir* **1993**, *9*, 9.
(13) Smit, B.; Hilbers, P. A. J.; Esselink, K.; Rupert, L. A. M.; van Os, N. M.; Schlijper, A. G. *Nature* **1990**, *348*, 624.
(14) Bolhuis P. G.; Frenkel, D. *Physisca A* **1997**, *244*, 45.
(15) Stillinger, F. H. *J. Chem. Phys.* **1983**, *78*, 4654.
(16) Wu, D.; Chandler, D.; Smit, B. *J. Phys. Chem.* **1992**, *96*, 4077.
(17) Floriano, M. A.; Caponetti, E.; Panagiotopoulos, A. Z. *Langmuir* **1999**, *15*, 3143.
(18) Larson, R. G.; Scriven, L. E.; Davis, H. T. *J. Chem. Phys.* **1985**, *83*, 2411.
(19) Larson, R. G. *J. Chem. Phys.* **1992**, *96*, 7904.
(20) Care, C. M.; Dalby, T. *Europhys. Lett.* **1999**, *45*, 38.
(21) Rodr×c1guez-Guadarrama, L. A.; Talsania, S. K.; Mohanty, K. K.; Rajagopalan, R. *Langmuir* **1999**, *15*, 437.
(22) Majhi, P. R.; Blume, A. *Langmuir* **2001**, *17*, 3844.
(23) Huibers, P. D. T.; Lobanov, V. S.; Katritzky, A. R.; Shah, D. O.; Karelson, M. *Langmuir* **1996**, *12*, 1462.
(24) Kusaka, I.; Oxtoby, D. W. *J. Chem. Phys.* **2001**, *115*, 4883.
(25) Marrink, S. J.; Tieleman, D. P.; Mark, A. E. *J. Phys. Chem. B* **2000**, *104*, 12165.
(26) Groot, R. D.; Warren, P. W. *J. Chem. Phys* **1997**, *107*, 4423.
(27) Groot, R. D. *Langmuir* **2000**, *16*, 7493.
(28) Karaborni, S.; van Os, N. M.; Esselink, K.; Hilbers, P. A. J. *Langmuir* **1993**, *9*, 1175.
(29) Frenkel, D.; Smit, B. *Understanding Molecular Simulation*, 2nd ed.; Academic Press: San Diego, CA, 2002.
(30) Hines, J. D. *Curr. Opin. Colloid Interface Sci.* **2001**, *6*, 350.
(31) Kofke, D. A.; Glandt, E. D. *Mol. Phys.* **1988**, *64*, 1105.
(32) Chandler, D. *Introduction to Modern Statistical Mechanics*; Oxford University Press: New York, 1987.
(33) Metropolis, N.; Rosenbluth, A. W.; Rosenbluth, M. N.; Teller, A. H.; Teller, E. *J. Chem. Phys.* **1953**, *21*, 1087.
(34) Duane, S.; Kennedy, A. D.; Pendleton, B. J.; Roweth, D. *Phys. Lett. B* **1987**, *195*, 216.
(35) Andersen, H. C. *J. Chem. Phys.* **1980**, *72*, 2384.
(36) Bearchell, C. A.; Heyes, D. M. *Phys. Chem. Chem. Phys.* **2001**, *3*, 5255.
(37) Andersen, H. C.; Weeks, J. D.; Chandler, D. *Phys. Rev. A* **1971**, *4*, 1597.
(38) Telo da Gama, M. M.; Gubbins, K. E. *Mol. Phys* **1986**, *59*, 227.
(39) Press: W. H.; Teukosky, S. A.; Vetterling, W. T.; Flannery, B. P. *Numerical Recipes in Fortran 77*; Cambridge University Press: Cambridge U.K., 2001.
(40) Giralco, L. A.; Good, R. J. *J. Phys. Chem.* **1957**, *61*, 904.
(41) Widom, B. *J. Chem. Phys.* **1963**, *39*, 2802.
(42) Merguro, K.; Takasawa, Y.; Kawahashi, N.; Tabata, Y.; Ueno, M. *J. Colloid. Interface Sci.* **1981**, *83*, 50.